Chapter 3
IRT Versus Moisture: Laboratory Tests

3.1 Aim

Several authors have used IRT to assess moisture (Balaras and Argiriou 2002; Avdelidis et al. 2003; Edis et al. 2014; Menezes et al. 2015); nevertheless, it is of most interest to evaluate its applicability in the laboratory, under controlled conditions, using full-scale models. Two situations were assessed: moisture intake due to rising damp and the drying process of a moist surface. In both cases, the passive approach was implemented as no external heat source was used. Moist areas were detected due to the effect of evaporative cooling at the surface.

A wall made of limestone blocks was selected as a case study to assess rising damp. The specimen was partially immersed in water for about 3 weeks, and thermal images were taken before and during the absorption period. To assess the drying process of a moist surface, a typical brick wall covered with painted rendering was sprayed with water on a limited area and thermal images were taken during the drying period, which lasted about 10 days. For the two phenomena, besides thermal images, a moisture detector was also used to qualitatively evaluate the moisture content of the walls.

3.2 Materials and Techniques

3.2.1 Set-up and Methodology

A full-scale limestone wall was used to assess raising damp. The specimen was partially immersed in 0.35 m of water for about 3 weeks. Measurements on the central area of the specimen (Fig. 3.1a) were carried out before the immersion period began (0 h) and 2, 4, 8, 28, 52, 100, 148, 196, 268, 340 and 532 h after the immersion.
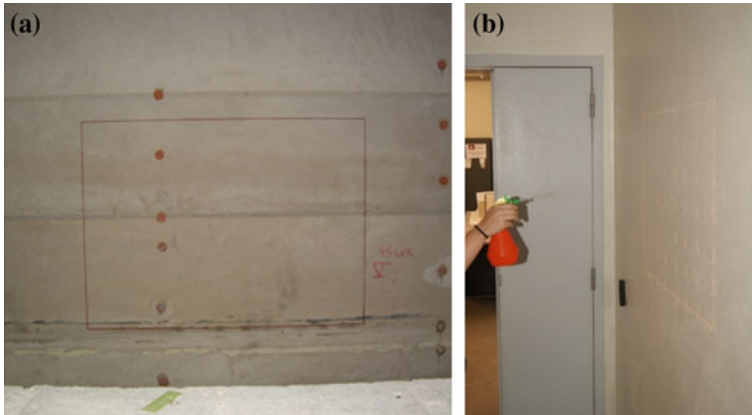
Fig. 3.1 a Area of the limestone wall used to assess rising damp; **b** area of the brick wall covered with painted rendering used to assess the drying process

A typical brick wall covered with painted rendering was used to assess the drying process of a moist surface. A limited area of the wall was sprayed three times with about 3 ml of water. The drying period took about 10 days. Measurements were carried out before spraying the surface, immediately after and every 15 min in the first hour. Additional measurements were also carried out 4, 28, 124 and 244 h after spraying the surface (Fig. 3.1b).

The measurements were performed using an IR camera, to assess the thermal patterns, and a moisture detector, to evaluate the relative moisture content of the walls. Throughout both tests, the IR camera was always kept in the same position. Average temperature and relative humidity in the laboratory during the test period were around 19 °C and 70%, respectively.

The moisture level above the water plan was also measured (stained/wet area), whenever the thermal images and the measurements with the moisture detector were carried out.

To compare the thermal images with the results of the moisture detector, a colour scale was proposed for the results of the detector. The warmer colours in the thermal image were linked to the lower values of the detector relative scale because in the dryer areas evaporation is less intense and therefore the surface temperature is higher (Fig. 3.2).

As the moisture detector only allows spot measurements and to guarantee a reliable comparison between the 2D thermal images and the results of the moisture detector, the area under study was divided into a grid. When assessing rising damp, the grid area was 0.78×0.45 m^2 and a total of 30 points were defined (Fig. 3.3a). To assess the drying process, the grid area was 0.70×0.60 m^2 and a total of 56 points were defined (Fig. 3.3b). Using the values measured at each point and the colour scale, a surface graph was created.
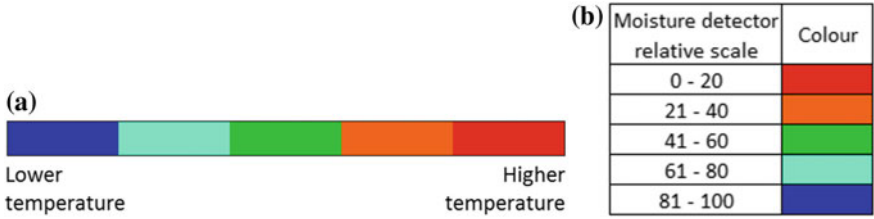
Fig. 3.2 a Thermal images colour scale (temperature in °C); **b** relative scale of the moisture detector and the corresponding colour scale
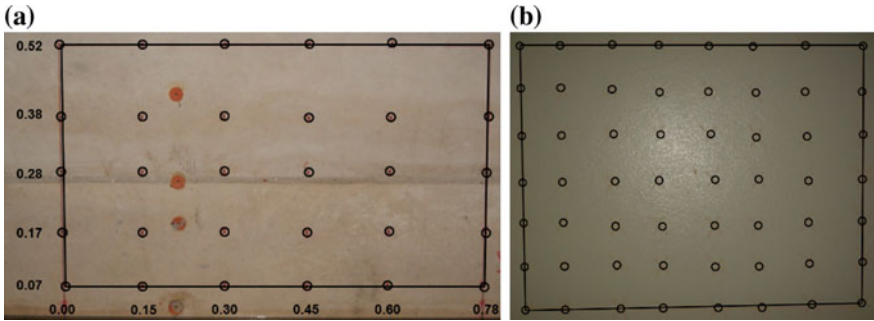

Fig. 3.3 a Grid of the area under study when assessing rising damp; **b** grid of the area under study when assessing the drying process

3.2.2 Equipment

Two different devices were used in this research: infrared camera (Fig. 3.4a) and moisture detector (Fig. 3.4b). The main specifications of the infrared camera are described in Table 3.1. The moisture detector is a non-destructive equipment that operates on the principle that the electrical impedance of a material varies in proportion to its moisture content. The instrument measures the electrical impedance of a material by creating a low-frequency alternating electric field between the electrodes. The reading displayed by the equipment is a relative scale in percentage, which indicates the greater or lesser signal (lower values indicate lesser signal that corresponds to lower moisture content).

Before the measurements were carried out, the calibration procedures were performed according to the operation manual of each device. Reflection calibration and ambient and background compensation of the infrared camera were assessed before each measurement.
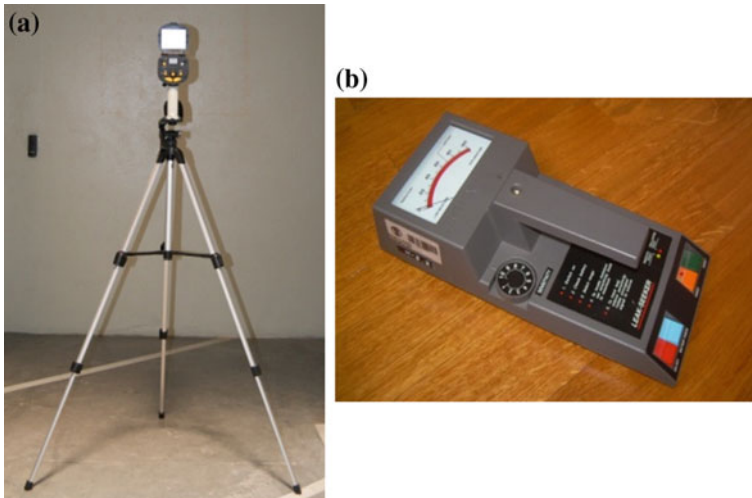
Fig. 3.4 Devices: **a** Infrared camera; **b** moisture detector

Table 3.1 Specifications of infrared camera

	Infrared camera
Measuring range	−20 to 100 °C
Resolution	0.1 °C
Accuracy	±2 °C or ±2% of reading
Detector	Uncooled focal plane array (microbolometer)
Spectral range	8–14 μm
Thermal image pixels	320 (H) × 240 (V) pixels
Focusing range	50 cm to infinite
IFOV	1.5 mrad

3.2.3 Materials

The dimensions of the limestone wall are $2.00 \times 1.85 \times 0.20 \text{ m}^3$, and it is composed of six blocks with 0.30 m height with horizontal mortar joints of about 1 cm thick (Fig. 3.1). The brick wall was covered with a cement-based plaster and finished with light coloured paint. The properties of the materials used in the models are presented in Table 3.2. More information about this specimen can be found in Guimarães et al. 2010.

Table 3.2 Properties of the
materials used in the models

Material	ε (−)	λ (W/m K)	ρ (kg/m^3)	c (J/kg K)
Limestone	0.88	0.723	2500	840
Mortar	0.93	1.37	1685	1000
Brick	0.86	0.60	1800	850
Paint	0.90	−		−

3.3 Results

3.3.1 Moisture Caused by Rising Damp

For evaluating rising damp, the highest visible moisture level above the water plan
was measured, whenever thermal images were taken and moisture content was mea-
sured. Figure 3.5 shows the time variation of the highest visible moisture level above
the water plan. A fast increase in the highest visible moisture level is visible in the
first 240 h, and afterwards, it remained approximately constant until the end of the
test. The stabilization occurred due to the equilibrium between the water intake and
the evaporation at the surface.

Figures 3.6, 3.7, 3.8, 3.9, 3.10, 3.11, 3.12, 3.13 and 3.14 show the evolution of the
moisture level in the specimen during the entire period of absorption (532 h) using
both the thermal images and the results of the moisture detector. Both the thermal
image and the measurement with the moisture detector show that the specimen was
dry before the humidification started (Fig. 3.6). Immediately after the tank was filled
with water (0.35 m of water above the bottom plan of the specimen), the water plan
can be detected in the thermal image as a colder area, limited by the black line in the
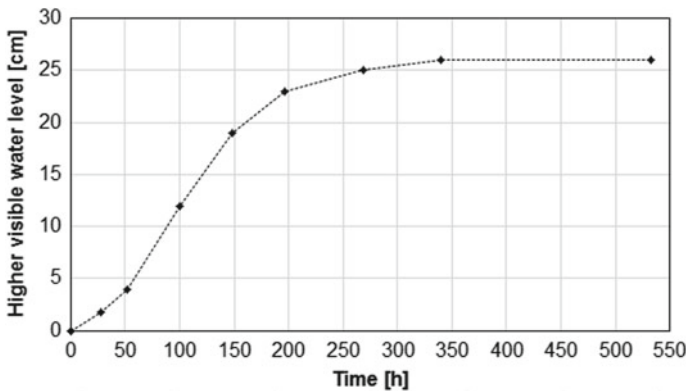image (Fig. 3.7).

Fig. 3.5 Time variation of the highest visible moisture level above the water plan
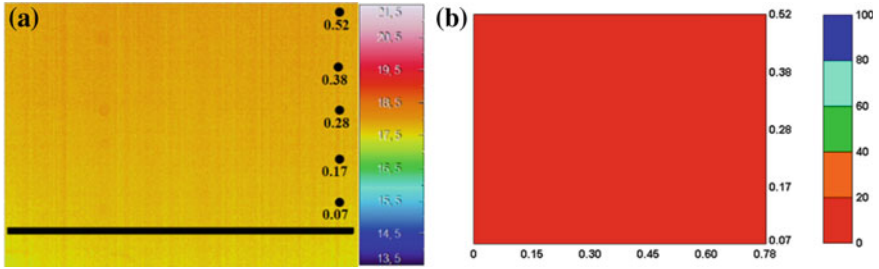
Fig. 3.6 Measurements before immersion began: **a** thermal image; **b** moisture detector results
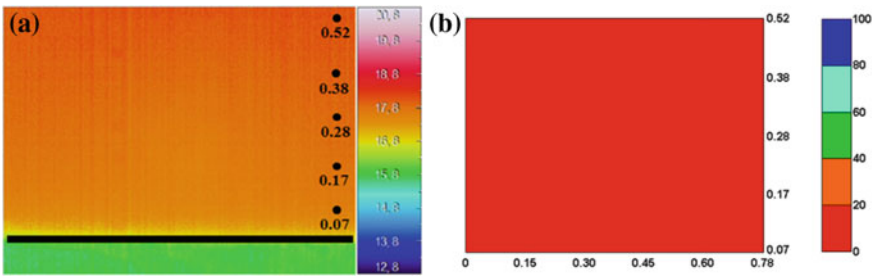

Fig. 3.7 Measurements immediately after the humidification began: **a** thermal image; **b** moisture detector results
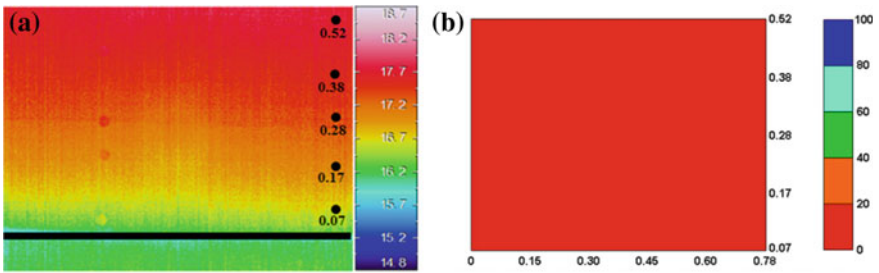

Fig. 3.8 Measurements 52 h after the imbibition began: **a** thermal image; **b** moisture detector results

At $t = 52$ h (Fig. 3.8), the highest moisture level above the water plan is about 0.04 m (Fig. 3.5), corresponding to the top of the green isothermal (Fig. 3.8a). The yellow isothermal shows the transition area between the wet and dry surfaces of the specimen. With the moisture detector (Fig. 3.8b), the rising damp was not identified yet because the moisture level has not reached the first row of the grid (0.07 m). About 2 days later, at $t = 100$ h, the thermal image shows that the top of the green isotherm is between the levels 0.07 and 0.17 m (Fig. 3.9a). This is supported both by the results of the moisture detector (Fig. 3.9b) and by the highest visible moisture level (Fig. 3.5).
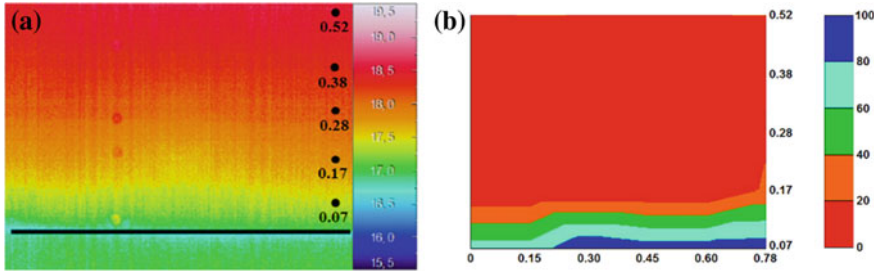
Fig. 3.9 Measurements 100 h after the imbibition began: **a** thermal image; **b** moisture detector results
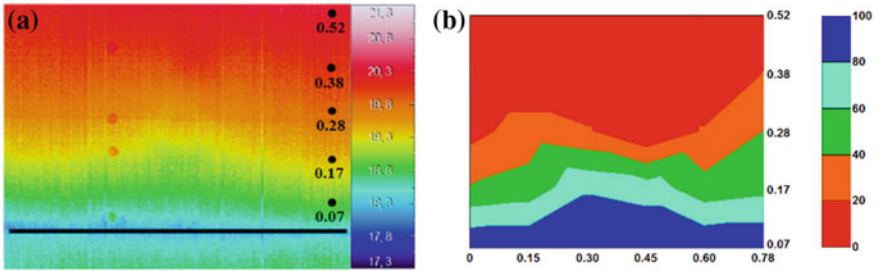

Fig. 3.10 Measurements 148 h after the imbibition began: **a** thermal image; **b** moisture detector results
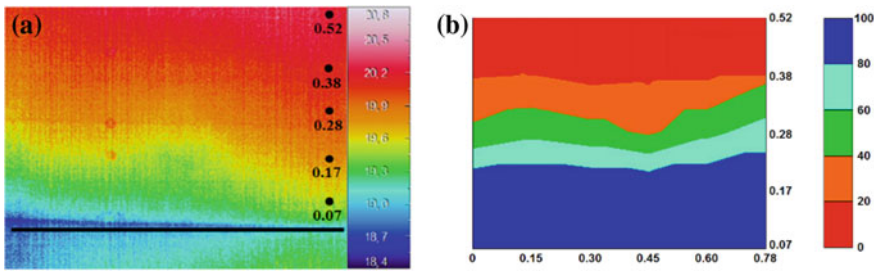

Fig. 3.11 Measurements 196 h after the imbibition began: **a** thermal image; **b** moisture detector results

Figures 3.10, 3.11, 3.12, 3.13 and 3.14 show that the thermal images point in the same direction as the results obtained with the moisture detector. Indeed, the moisture level assessed by both methods is quite similar. The thermal images also show that the moisture level is higher in the centre of the specimen and lower near the verticals corners, which was not visually perceptible. This phenomenon can be explained by the effect of more intense rising damp evaporation near the corners of the specimen.
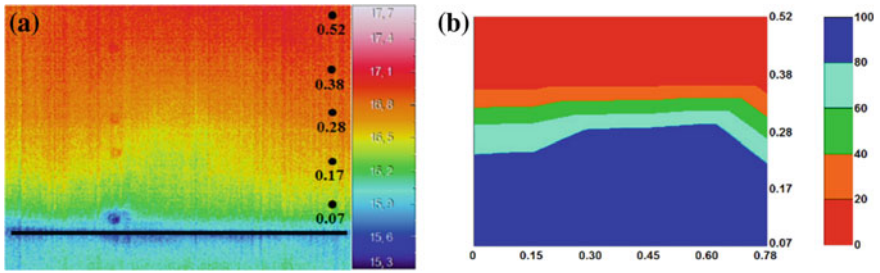
Fig. 3.12 Measurements 268 h after the imbibition began: **a** thermal image; **b** moisture detector results
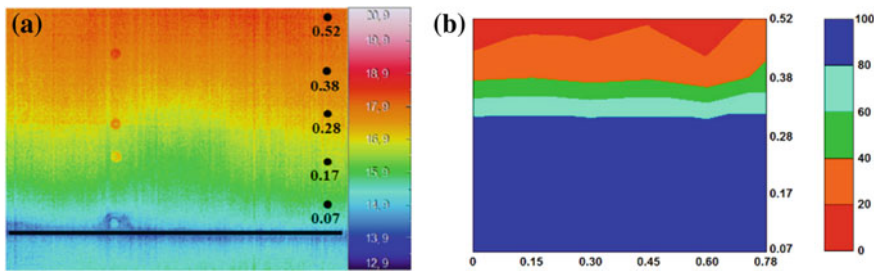

Fig. 3.13 Measurements 340 h after the imbibition began: **a** thermal image; **b** moisture detector results
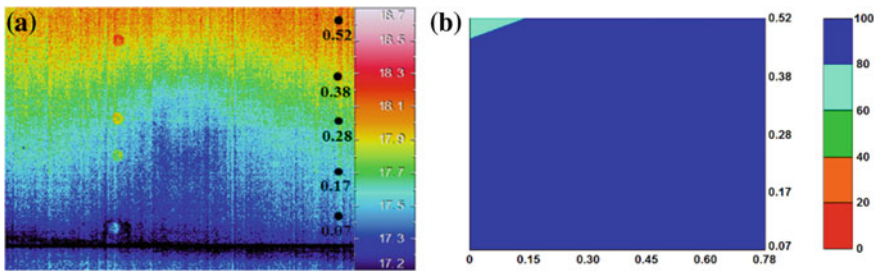

Fig. 3.14 Measurements 532 h after the imbibition began: **a** thermal image; **b** moisture detector results

At the end of the measurement, the results of the moisture detector (Fig. 3.14b) show that the level of the moist area (dark blue) is above 0.52 m, while in the thermal image (Fig. 3.14a), it is around 0.38 m. Also, the difference between the thermal images in Figs. 3.13a and 3.14a are not very relevant, pointing to a stabilization of the moisture level. On the other hand, when analysing the results of the moisture detector, a more pronounced difference can be found. Although these results are not completely in accordance, they are expectable. In fact, IRT only detects surface evaporation and the moisture detector assesses inner moist (around 2 cm penetration
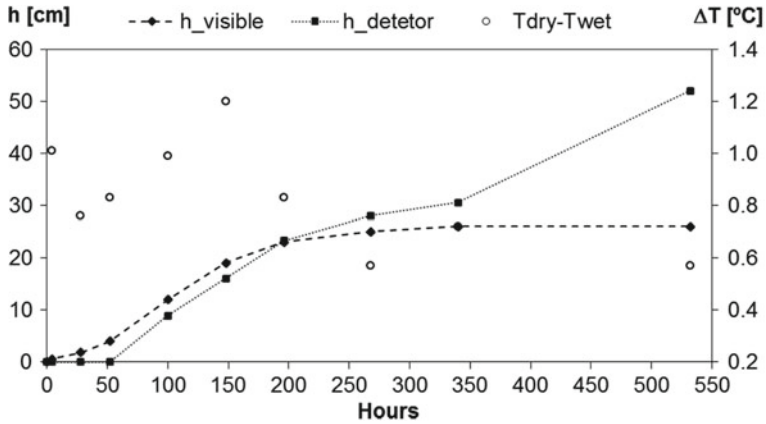
Fig. 3.15 Time variation of the highest visible moisture level above the water plan (h_visible), the highest moisture level above the water plan measured by the moisture detector (h_detector) and the temperature difference between the dry and wet areas (Tdry-Twet)

depth). This is also in line with the results of the numerical simulation performed by Guimarães et al. (2010), showing that the moisture level at the surface is lower than inside the specimen, because evaporation is more preponderant than capillarity, which allows the stabilization of the superficial moisture level. Inside the specimen, capillarity remains the main driving force and the moisture level keeps increasing.

Figure 3.15 shows the time variation of the highest visible moisture level above the water plan (h_visible), the highest moisture level above the water plan measured by the moisture detector (h_detector) and the temperature difference between the dry and wet areas (Tdry-Twet) calculated from the thermal images. The results indicate that the temperature difference increases until 148 h after the start of the humidification and then decreases, becoming stable after approximately 268 h, with a value around 0.6 °C. The temperature gradient starts decreasing when the visible moisture level above the water plan starts stabilizing at around 25 cm ($t = 196$ h), which means that IRT is more efficient when the capillarity phenomenon is more intense.

The level of rising damp measured by the moisture detector follows the trend of the visible level and of the temperature difference until $t = 268$ h. After that instant, it continues increasing until the hygric equilibrium is achieved. The higher level of the rising damp measured with the moisture detector was expected as IRT only detects surface evaporation and the moisture detector assesses inner moist. Further analysis concerning this specific issue can be found in Barreira et al. (2016). These results are in line with the ones obtained by Camino et al. (2014), although in their work moisture has been assessed through a destructive methodology.
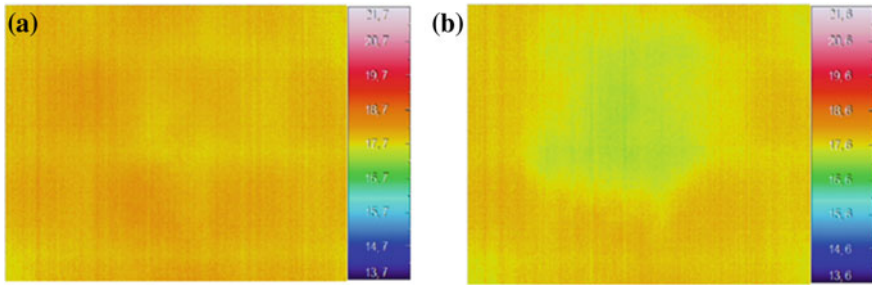
Fig. 3.16 Thermal image taken to assess surface condensation: **a** before spraying the surface; **b** immediately after spraying the surface
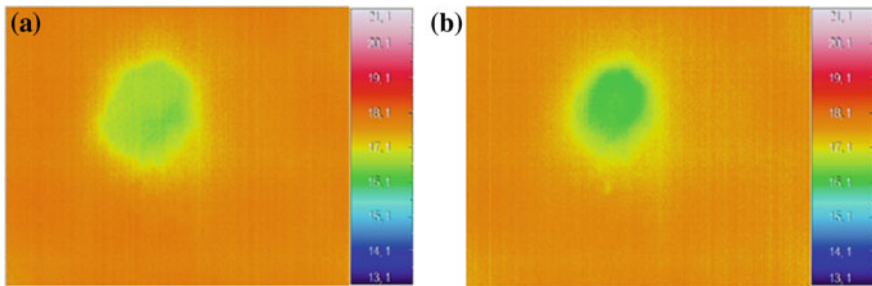

Fig. 3.17 Thermal image taken to assess surface condensation: **a** 15 min after spraying the surface; **b** 30 min after spraying the surface

3.3.2 Drying Process

To assess the drying process, a typical brick wall covered with painted rendering was used. Figures 3.16, 3.17, 3.18, 3.19 and 3.20 show the thermal images taken before and immediately after the spraying and during the drying period. Figure 3.16a shows that the wall was dry before it was sprayed with water. This conclusion is also supported by the results of the moisture detector (Fig. 3.21a).

After spraying the surface, the moist area was immediately detected on the thermal images through a limited colder area, which indicates a more intense evaporation. This area decreased during the drying process, especially in the first hour. Also, the temperature difference between the wet and dry areas decreases over time. After the first hour, the stained area was hardly visually detected and could only be detected through IRT. At the end of the test, no stained area could be detected in the thermal image (Fig. 3.20b).

The results of the moisture detector during the drying process were not reliable as no moisture was detected. In fact, the results obtained before spraying the surface and immediately after (Fig. 3.21) are very similar and do not indicate the presence
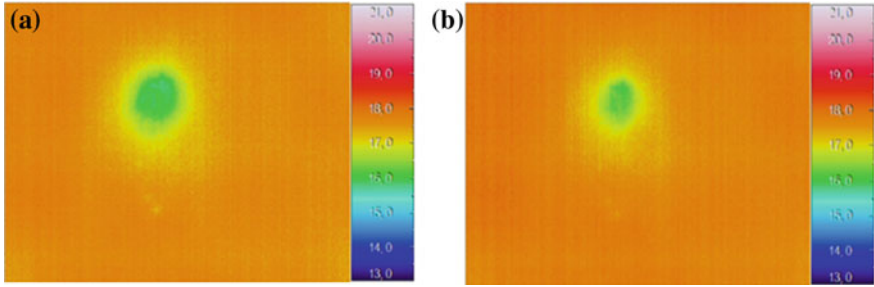
Fig. 3.18 Thermal image taken to assess surface condensation: **a** 45 min after spraying the surface; **b** 1 h after spraying the surface
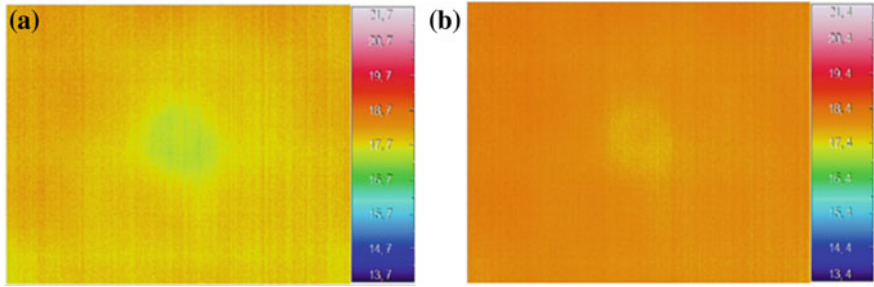

Fig. 3.19 Thermal image taken to assess surface condensation: **a** 4 h after spraying the surface; **b** 28 h after spraying the surface
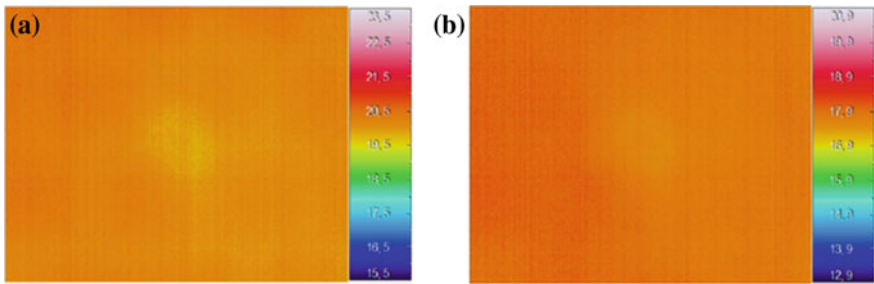

Fig. 3.20 Thermal image taken to assess surface condensation: **a** 124 h after spraying the surface; **b** 244 h after spraying the surface

of any moisture. Yet, this result was already expected, since the moisture detector only assesses inner moist.

Figures 3.22 and 3.23 show the time variation of the relative moist area (ratio between moist and dry area) and the difference between the maximum temperature (on the dry area) and minimum temperature (on the moist area).
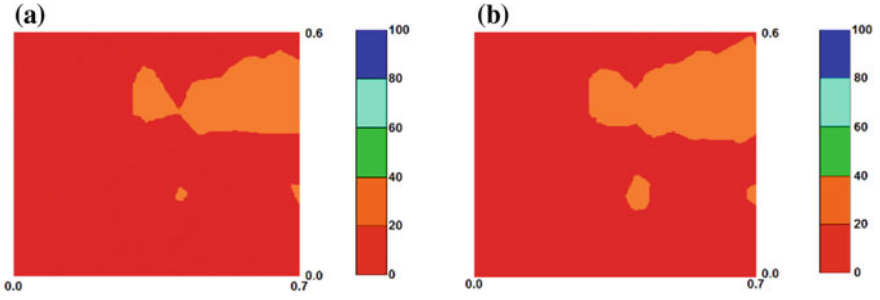
Fig. 3.21 Results of the moisture detector when assessing surface condensation: **a** before spraying the surface; **b** immediately after spraying the surface
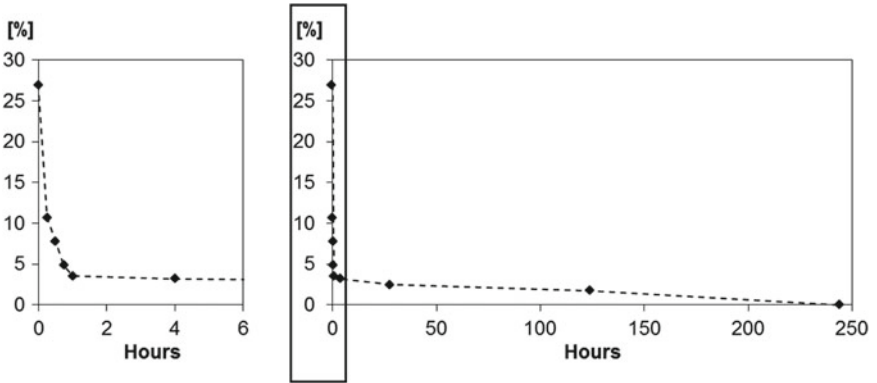

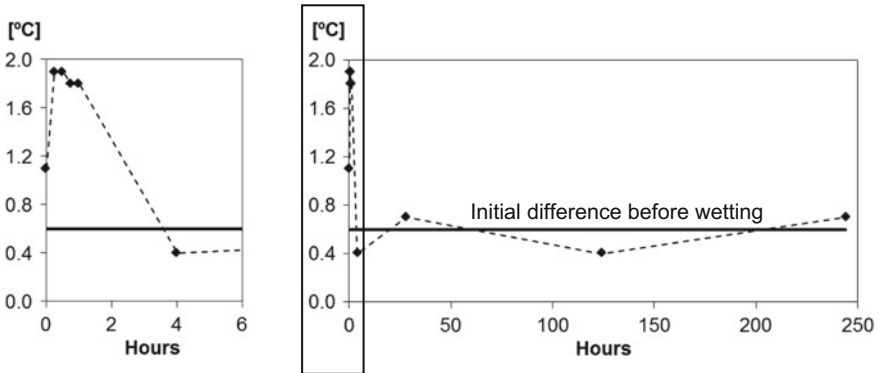**Fig. 3.22** Time variation of the relative moist area (ratio of moist and dry area)

Fig. 3.23 Time variation of the difference between the maximum temperature (on the dry area) and minimum temperature (on the moist area)

The results point in the same direction of the qualitative analysis. Indeed, the stained area due to moisture decreased throughout the period of analysis, and the higher variations occurred in the first hour. After that period, the relative moist area was lower than 3.5%, indicating a stabilization of the drying process as no relevant deviations can be found (Fig. 3.22).

The temperature difference between the dry and wet areas (Fig. 3.23) was used to assess the drying process. The results confirm that the first hour was the most import. In fact, temperature differences were around 2 °C in the first hour, dropping to around 0.6 °C, which was the difference measured before the wetting process. It must be stated that there was an increase in the temperature difference in the first 15 min of drying that may be related to the intensity of water evaporation at the surface, which was lower immediately after spraying the surface.

3.4 Discussion of the Results

A new approach based on a common colour scale was applied both in IRT and in moisture readings and was tested on full-scale experimental set-ups. With this procedure, the IRT potential to assess moist areas due to capillarity and during the drying process was highlighted. Specific situations that cannot be visually detected were identified by IRT as the transition between the wet and dry surfaces of the specimens.

When assessing rising damp, generally, there is a good agreement between the thermal images and the readings of the moisture detector. However, the moisture detector points to a higher level of moisture, because IRT only detects surface evaporation, while the moisture detector assesses inner moisture. This is in accordance with numerical simulation performed by other authors, whose results confirm that the moisture level at the surface is lower than at mid-thickness of the specimen.

When evaluating the drying process, it was not possible to achieve an agreement between IRT and the moisture detector, because only superficial moisture was assessed and, therefore, the moisture detector was not able to detect it. However, IRT allowed understanding the critical period for the drying, not only in terms of stained area but also when assessing temperature differences between the stained and dried areas.

References

Avdelidis N, Moropoulou A, Theoulakis P (2003) Detection of water deposits and movement in porous materials by infrared imaging. Infrared Phys Technol 44(3):183–190

Balaras C, Argiriou A (2002) Infrared thermography for building diagnostics. Energy Build 34(2):171–183

Barreira E, Almeida RMSF, Delgado JMPQ (2016) Infrared thermography for assessing moisture related phenomena in building components. Constr Build Mater 110:251-69

Camino MS, León FJ, Llorente A, Olivar JM (2014) Evaluation of the behavior of brick tile masonry and mortar due to capillary rise of moisture. Mater Constr 64(314)

Edis E, Flores-Colen I, Brito J (2014) Passive thermographic detection of moisture problems in façades with adhered ceramic cladding. Constr Build Mater 51:187–197

Guimarães AS, Delgado JMPQ, Freitas VP (2010) Mathematical analysis of the evaporative process of a new technological treatment of rising damp in historic buildings. Build Environ 45(11):2414–2420

Menezes A, Gomes MG, Flores-Colen I (2015) In-situ assessment of physical performance and degradation analysis of rendering walls. Constr Build Mater 75:283–292